Analyses of the P-V and V-Q curves for a power system with UPFC

Okon Tomasz, Wilkosz Kazimierz, Lukomski Robert

Abstract
The paper deals with the system P-V or V-Q curves utilized for stability analyses of a power system. The determination of the mentioned nose curves is considered for a power system which is equipped with an Unified Power Flow Controller (UPFC). In the paper, a comparison of calculation for a power system with and without the UPFC device is made. When the power system with the UPFC device is modelled the controlled sources have to be taken into account. To achieve suitably high influence of the UPFC device on behaviour of a power system, proper parameters of UPFC should be chosen. This is the main problem considered in the paper.

Keywords: Power System, Stability, UPFC

Introduction

From the view-point of power system operation, voltage instability is recognised as one of the major problems [1]. Among factors contributing to this problem are (i) decreasing the number of voltage controlled points and increasing the electrical distance between generation and load because of the building of larger, remote power plants, (ii) the instability point is closer to normal values as a result of the heavy use of shunt compensation to support the voltage profile, (iii) relatively large probability of occurrence of tripping of transmission or generation equipment, (iv) in the transmission open access environment, existence of economical incentive to operate power systems closer to their limits. It becomes very essential to determine the conditions in which voltage instability can occur.

It is common to consider the curves which relate voltage to active or reactive power, i.e. the curves P-V or V-Q, called also as nose curves, for the aim of voltage instability analyses.

The aim of the paper is to present results of analyses of the curves P-V and V-Q for a power system in which the Unified Power Flow Controller (UPFC) is installed. The UPFC device is one of the FACTS devices, which enables flexible control of a power system [2]. During investigations of the curves P-V and V-Q, different values of parameters of UPFC and constraints on operation of the UPFC device are taken into account.

CHARACTERISTICS OF UPFC

The UPFC device in its general form can provide simultaneous, real-time control of all basic power system parameters (transmission voltage, impedance, and phase angle), or any combinations thereof, determining the transmitted power [2].

UPFC consists of two switching converters. These converters are voltage sourced inverters using gate turn-off (GTO) thyristor valves. The inverters are labelled as *Inverter 1* and *Inverter 2* in Fig. 1. They are coupled with common DC-link (provided by a DC storage capacitor) which allows free exchanging real power between the inverters. *Inverter 1*, which is connected with a transmission line through shunt transformer, is to supply or absorb a real power demand of *Inverter 2* by the common DC link. *Inverter 2* is coupled with the transmission line through a series transformer and provides the principle function by injecting an AC voltage with a controllable magnitude and a phase angle. Each inverter can independently generate or absorb reactive power at its own AC output terminal.

The model of UPFC shown in Fig. **2** is composed of two controllable ideal voltage-sources [3]. These two coordinated synchronous voltage sources represent the UPFC adequately for the purpose of fundamental frequency steady-state analysis.

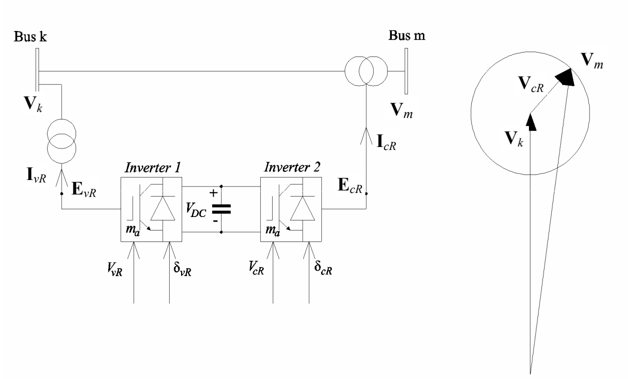

Fig.1 UPFC using two voltage-sourced inverters with a direct voltage link.

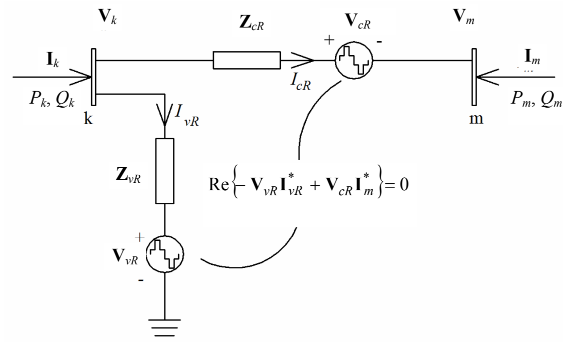

Fig.2 Equivalent circuit based on solid-state voltage sources. $\mathbf{V}_{vR}=V_{vR}(\cos\delta_{vR}+j\sin\delta_{vR})$ **,** $\mathbf{V}_{cR}=V_{cR}(\cos\delta_{cR}+j\sin\delta_{cR})$

Taking into account the equivalent circuit shown in Fig. 2 we can derive the equations:

For bus *k*:

$$P_k=V_k^{\,2}G_{kk}+V_kV_m\left[G_{km}\cos(\theta_k-\theta_m)+B_{km}\sin(\theta_k-\theta_m)\right]+ +V_kV_{cR}\left[G_{km}\cos(\theta_k-\delta_{cR})+B_{km}\sin(\theta_k-\delta_{cR})\right]+ +V_kV_{vR}\left[G_{vR}\cos(\theta_k-\delta_{vR})+B_{vR}\sin(\theta_k-\delta_{vR})\right], \quad (1)$$

$$Q_k=-V_k^{\,2}B_{kk}+V_kV_m\left[G_{km}\sin(\theta_k-\theta_m)-B_{km}\cos(\theta_k-\theta_m)\right]+ +V_kV_{cR}\left[G_{km}\sin(\theta_k-\delta_{cR})-B_{km}\cos(\theta_k-\delta_{cR})\right]+ +V_kV_{vR}\left[G_{vR}\sin(\theta_k-\delta_{vR})-B_{vR}\cos(\theta_k-\delta_{vR})\right] \quad (2)$$

For bus m:

$$P_m=V_m^{\,2}G_{mm}+V_mV_k\left[G_{mk}\cos(\theta_m-\theta_k)+B_{mk}\sin(\theta_m-\theta_k)\right]+ +V_mV_{cR}\left[G_{mm}\cos(\theta_m-\delta_{cR})+B_{mm}\sin(\theta_m-\delta_{cR})\right] \quad (3)$$

$$Q_m=-V_m^{\,2}B_{mm}+V_mV_k\left[G_{mk}\sin(\theta_m-\theta_k)-B_{mk}\cos(\theta_m-\theta_k)\right]+ +V_mV_{cR}\left[G_{mm}\sin(\theta_m-\delta_{cR})-B_{mm}\cos(\theta_m-\delta_{cR})\right] \quad (4)$$

For series inverter:

$$P_{cR}=V_{cR}^{\,2}G_{mm}+V_{cR}V_k\left[G_{km}\cos(\delta_{cR}-\theta_k)+B_{km}\sin(\delta_{cR}-\theta_k)\right]+ +V_{cR}V_m\left[G_{mm}\cos(\delta_{cR}-\theta_m)+B_{mm}\sin(\delta_{cR}-\theta_m)\right] \quad (5)$$

$$Q_{cR}=-V_{cR}^{\,2}B_{mm}+V_{cR}V_k\left[G_{km}\sin(\theta_{cR}-\theta_k)-B_{km}\cos(\theta_{cR}-\theta_k)\right]+ +V_{cR}V_m\left[G_{mm}\sin(\theta_{cR}-\theta_m)-B_{mm}\cos(\theta_{cR}-\theta_m)\right] \quad (6)$$

For shunt inverter:

$$P_{vR}=-V_{vR}^{2}G_{vR}+V_{vR}V_k\left[G_{vR}\cos(\delta_{vR}-\theta_k)+B_{vR}\sin(\delta_{vR}-\theta_k)\right] \quad (7)$$

$$Q_{vR}=V_{vR}^{2}B_{vR}+V_{vR}V_k\left[G_{vR}\sin(\delta_{vR}-\theta_k)-B_{vR}\cos(\delta_{vR}-\theta_k)\right] \quad (8)$$

where:

P, *Q* denote active and reactive power respectively,

$$\mathbf{Y}_{kk}=G_{kk}+jB_{kk}=\mathbf{Z}_{cR}^{-1}+\mathbf{Z}_{vR}^{-1},$$
$$\mathbf{Y}_{mm}=G_{mm}+jB_{mm}=\mathbf{Z}_{cR}^{\;-1},$$
$$\mathbf{Y}_{km}=\mathbf{Y}_{mk}=G_{km}+jB_{km}=-\mathbf{Z}_{cR}^{\;-1},$$
$$\mathbf{Y}_{vR}=G_{vR}+jB_{vR}=-\mathbf{Z}_{vR}^{\;-1}.$$

Neglecting UPFC losses, we can state that UPFC cannot absorb and injects real power, i.e. the active power supplied to the shunt converter, P_{vR}, equals the active power demanded by the series converter, P_{cR}:

$$P_{bb}=P_{vR}+P_{cR}=0\,. \quad (9)$$

The earlier-presented model of UPFC was implemented in a computer program for calculation of power flows. The algorithm for power flows uses the Newton-Raphson method [5]. Using the mentioned program we can investigate such functions of the UPFC device as setting: (i) a power flow in the transmission line where UPFC is installed, (ii) a voltage magnitude at the selected bus of a power network, (iii) difference between phase angles of the voltages at the ending bus of the transmission line with UPFC, (iv) a level of compensation of the reactance of the mentioned transmission line. The described results of the utilization of the UPFC device are achieved by appropriate change of the magnitudes and the angles of the source voltages of the UPFC series and shunt sources.

DESCRIPTION OF THE CARRIED OUT INVESTIGATIONS

Assumptions

It was assumed that:

1. In the investigations, the 5-bus test system [5] (Fig. **3**) is utilized. The parameters of the test system with UPFC are as it is presented in Table 1 and Table 2. In the test system, *Bus 1* is a slack bus, and *Bus 2* is a *PV* bus.
2. In the investigations, two cases are considered: (i) in the test system there is no a UPFC device, (ii) in the test system there is a UPFC device.
3. The UPFC device is modelled as it is presented in the previous section.
4. If in the test system there is UPFC, it regulates the voltage at *Bus 3* with a target voltage equal to 1.0 p.u. and also it changes an equivalent reactance (compensates the transmission line) between *Bus 3* and *Bus 4* (Fig. 4).
5. The *P-V* and *V-Q* analyses are carried out for *Bus 4* in the test system.
6. The reactive load at *Bus 4* when the *P-V* analysis is carried out and the active load at *Bus 4*, when the *V-Q* analysis is carried out, are the same as in the reference point of operation of the test system, i.e.:
   - the reactive load at *Bus 4* is equal to 0.05 p.u.,
   - the active load at *Bus 4* is equal to 0.4 p.u.
7. In the investigations, when in the test system there is the UPFC device, the parameters X_{cr}, X_{vr} ($\mathbf{Z}_{cr}=j\,X_{cr}$, $\mathbf{Z}_{vr}=j\,X_{vr}$) of the UPFC device are changed and constraints for the magnitudes of the source voltages of the UPFC series and shunt source are considered.

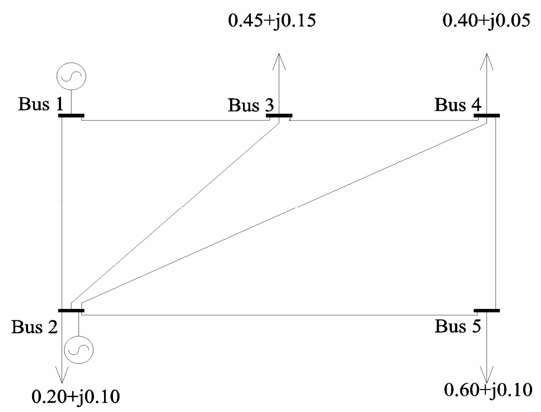

Fig.3 The 5-bus test system

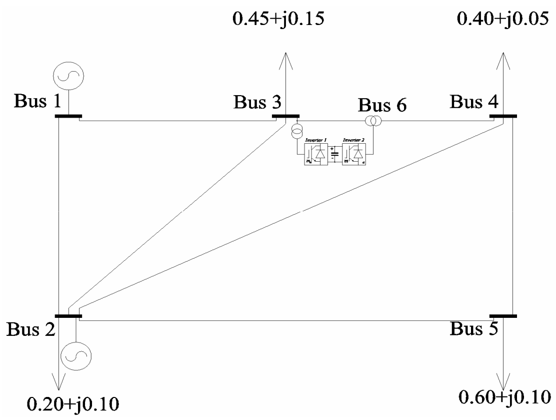

Fig.4 The 5-bus test system with UPFC

Line No.	Node 1	Node 2	R p.u.	X p.u.	G p.u.	B p.u.
1	1	2	0.02	0.06	0	0.06
2	1	3	0.08	0.24	0	0.05
3	2	3	0.06	0.18	0	0.04
4	2	4	0.06	0.18	0	0.04
5	2	5	0.04	0.12	0	0.03
6	6	4	0.01	0.03	0	0.02
7	4	5	0.08	0.24	0	0.05

Tab.1 Parameters of the lines of the test system with UPFC

Node	Type	P_G p.u.	Q_G p.u.	P_L p.u.	Q_L p.u.
1	1	-	-	-	-
2	2	0,4	-	0,20	0,10
3	3	-	-	0,45	0,15
4	3	-	-	0,40	0,05
5	3	-	-	0,60	0,10
6	3	-	-	-	-

Tab.2 Generations and loads for different nodes of the test system with UPFC for the reference operation point

P-V and V-Q curves

Results of investigations of the *P-V* and *V-Q* curves for the case when there is no UPFC in the test system (the dashed line) and for the case when there is UPFC in the test system (the solid line) are presented in the figures: Fig. 5 – Fig. 11.

In Fig. 5 – Fig. 11, there are results of the investigations for the following cases: Fig. 5 – Fig. 7 - $X_{cr} = X_{vr} = 0.1$ p.u., Fig. 8 – Fig. 9 - $X_{cr} = X_{vr} = 0.05$ p.u., Fig. 10 – Fig. 11 - $X_{cr} = X_{vr} = 0.01$ p.u. The constraints for the magnitude of the source voltage of the UPFC shunt source is in the range: [0.9, 1.1] p.u. – Fig. 6, Fig. 8, Fig. 10 or [0.5, 1.5] p.u. – Fig. 7, Fig. 9, Fig. 11. The magnitude of the source voltage of the UPFC series source is constrained by the value of 0.2 p.u.

The calculations show the visible dependence of the nose curves *P-V* and *V-Q* on parameters X_{cr}, X_{vr} and constraints which are considered in the investigations, i.e. on constraints for the UPFC series and shunt source voltage.

When there are no constraints for the magnitudes of the source voltages of the UPFC series and shunt source, we have the nose curves which are the continuous ones and these curves are determined for the whole considered range of the voltage magnitude at *Bus 4*. When there are any constraints for magnitudes of the source voltages of the sources in the UPFC model, both the *P-V* and *V-Q* nose curves can not be determined for the whole range of the voltage magnitude at *Bus 4*. The voltage magnitude at *Bus 4* can not have certain values. It is easy to observe that the range of such values of the voltage magnitude at the *Bus 4* changes as the constraints on the voltage magnitude for the UPFC shunt source change.

Fig. 5 shows that if there are no constraints for UPFC, then the magnitude of the voltage at *Bus 4* decreases slower than in the case of lack of UPFC when active power increases and reactive power is equal to 0.05 p.u. The slower changes of the voltage at *Bus 4* is a consequence of the existence of UPFC. When active power is equal to 0.4 p.u. and reactive power changes the voltage magnitude at *Bus 4* changes faster than in the case of lack of UPFC. The reason are relatively-high values of X_{cr} and X_{vr} comparing with a reactance of the line between *Bus 6* and *Bus 4*. In this situation, the influence of UPFC on the *V-Q* nose curve is reduced.

In Fig. 6, there are the *P-V* and *V-Q* nose curves for the test system with the UPFC device for a case when there are no constraints and for a case when there are such constraints for UPFC. In the second case, for certain values of power, the voltage magnitude at *Bus 4* changes faster with changes of active power (the *P-V* curve) or with changes of reactive power (the *V-Q* curve) than in the first case. When there are constraints for UPFC the features of the test system are worse from the view-point of stability.

Analyzing results of investigations presented in Fig. 7 – 11, one can ascertain that for lower values of X_{cr} and X_{vr} changes of the voltage magnitude at *Bus 4* considered as function of active power (the *P-V* curve) are smaller. The same situation is, when we take into account the *V-Q* curves. Additionally, in the case of the *V-Q* curves we can observe that beginning from certain values of X_{cr} and X_{vr}, changes of the voltage magnitude at *Bus 4* are smaller than in the case of the system without UPFC. The presented observations point out that utilization of UPFC improves features of the power system.

Conclusion

The UPFC device is one of the FACTS devices. These devices are utilized for control of power systems. The effect of utilization of UPFC can be different in dependence of parameters of this device. The investigations show that changes of values of such parameters of equivalent circuit of UPFC as X_{cr} and X_{vr} have essential influence on features of a power system. When the values of X_{cr} and X_{vr} are smaller, the features of a power system are better. The voltage magnitude at a distinguished node changes less in dependence of changes of active or reactive load. Generally, we can state that decreasing the values of X_{cr} and X_{vr} improves stability features of a power system. The other conclusion is that to achieve suitably high influence of UPFC on features of a power system the relation among the values of X_{cr} and X_{vr} and parameters of the power line, where UPFC is installed, should be properly chosen.

The carried out investigations show, that there is visible dependence between the curves *P-V* and *V-Q* and the constraints on source voltages of sources occurring in the model of the UPFC device. These constraints can essentially modify the curves *P-V* and *V-Q*, comparing to those situation when there are no such constraints.

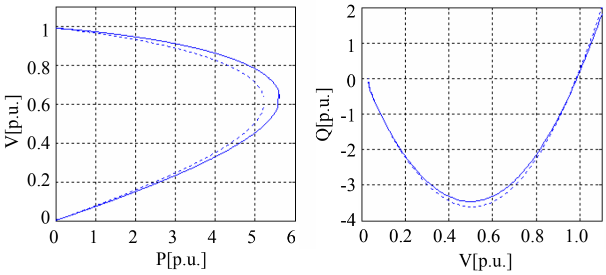

Fig.5 **The nose curves a) *P-V*, b) *V-Q* for *Bus 4* in the test system.**
—— the test system with UPFC, $X_{cr} = X_{vr} = 0.1$ p.u., there are no constraints for the UPFC shunt source; ······· the test system without UPFC

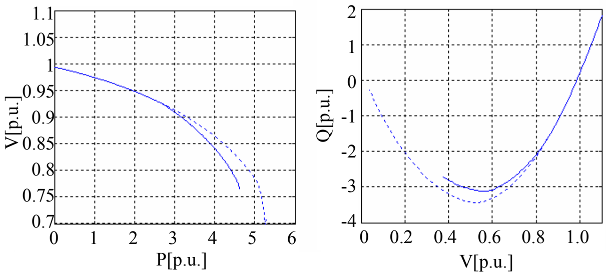

Fig.6 **The nose curves a) *P-V*, b) *V-Q* for *Bus 4* in the test system when when $X_{cr} = X_{vr} = 0.1$ p.u.**
—— the test system with UPFC when the voltage magnitude of the UPFC shunt source is in the range [0.9, 1.1] p.u.; ······· the test system with UPFC when there are no constraints for UPFC

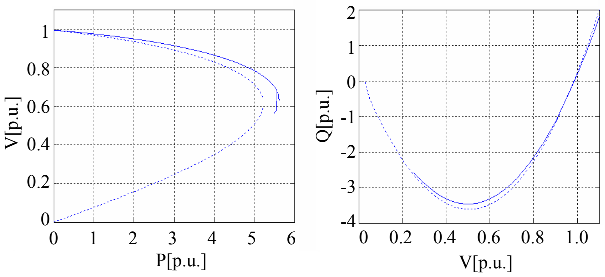

Fig.7 **The nose curves a) *P-V*, b) *V-Q* for *Bus 4* in the test system.**
—— the test system with UPFC, $X_{cr} = X_{vr} = 0.1$ p.u. and the voltage magnitude of the UPFC shunt source is in the range [0.5, 1.5] p.u.; ······· the test system without UPFC

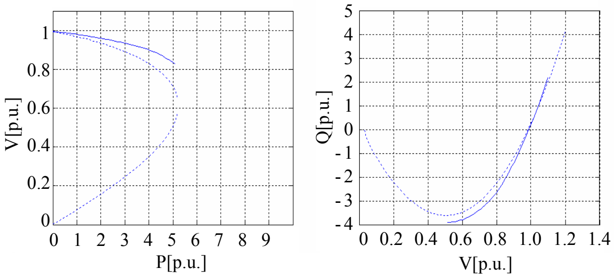

Fig.8 **The nose curves a) *P-V*, b) *V-Q* for *Bus 4* in the test system.**
—— the test system with UPFC, when $X_{cr} = X_{vr} = 0.05$ p.u. the voltage magnitude of the UPFC shunt source is in the range [0.9 1.1] p.u.; ······· the test system without UPFC

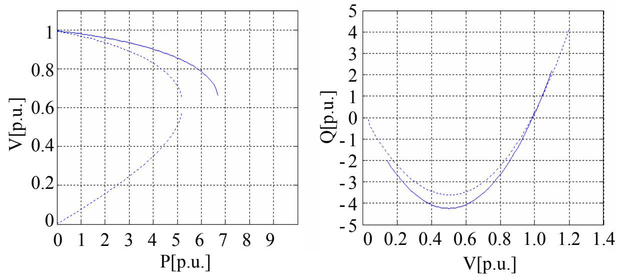

Fig.9 **The nose curves a) *P-V*, b) *V-Q* for *Bus 4* in the test system.**
—— the test system with UPFC, when $X_{cr} = X_{vr} = 0.05$ p.u., the voltage magnitude of the UPFC shunt source is in the range [0.5 1.5] p.u.; ······· the test system without UPFC

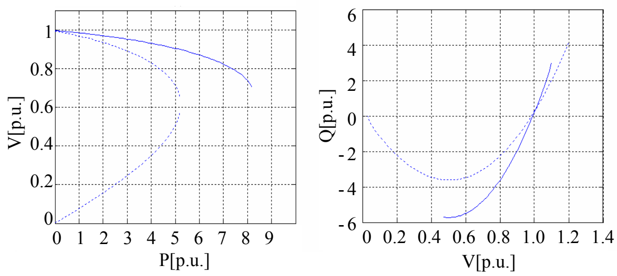

Fig.10 **The nose curves a) *P-V*, b) *V-Q* for *Bus 4* in the test system.**
—— the test system with UPFC, when $X_{cr} = X_{vr} = 0.01$ p.u. the voltage magnitude of the UPFC shunt source is in the range [0.9 1.1] p.u.; ······· the test system without UPFC

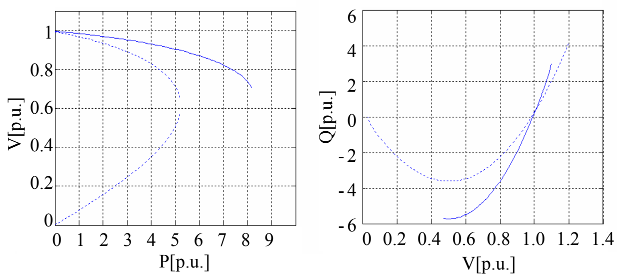

Fig.11 **The nose curves a) *P-V*, b) *V-Q* for *Bus 4* in the test system,**
—— the test system with UPFC, when $X_{cr} = X_{vr} = 0.01$ p.u. the voltage magnitude of the UPFC shunt source is in the range [0.5 1.5] p.u.; ······· the test system without UPFC

References

[1] Van Cutsem, T. (2000): Voltage instability: phenomena, countermeasures, and analysis methods, Proceedings of the IEEE, Vol 88, No 5, 208-227.

[2] Gyugyi, L. (1992): Unified power-flow control concept for flexible AC transmission systems, IEE Proceedings C Generation, Transmission and Distribution, Vol. 139, No. 4, 323 – 331.

[3] Nabavi-Niaki, A.; Iravani, M.R. (1996): Steady-state and dynamic models of unified power flow controller (UPFC) for power system studies. IEEE Transactions on Power Systems, Vol. 11, No. 4, 1937 – 1943.

[4] Acha, E., Fuerte-Esquivel, C.R. (1997): Unified power flow controller: a critical comparison of Newton-Raphson UPFC algorithms in power flow studies. IEE Proc.-Gen. Transm. Distrib., Vol. 144, No. 5, 437-444.

[5] Fuerte-Esquivel, C.R. Acha, E., Ambriz-Perez H. (2000): A Comprehensive Newton-Raphson UPFC Model for Quadratic Power Flow Solution of Practical Power Networks. IEEE Transaction on Power Systems, Vol. 15, No.1, 102-109.

Mr. Tomasz Okon

Wroclaw University of Technology
Electrical Engineering Faculty
Electrical Power Engineering Institute
Wybrzeze Wyspianskiego 27
50-370 Wroclaw, Poland
Fax: +48 71 3202656
E-mail: tomasz.okon@pwr.wroc.pl

Prof. Kazimierz Wilkosz, Ph.D., D. Sc.

Wroclaw University of Technology
Electrical Engineering Faculty
Electrical Power Engineering Institute
Wybrzeze Wyspianskiego 27
50-370 Wroclaw, Poland
Fax: +48 71 3202656
E-mail: kazimierz.wilkosz@pwr.wroc.pl

Dr. Robert Lukomski

Wroclaw University of Technology
Electrical Engineering Faculty
Electrical Power Engineering Institute
Wybrzeze Wyspianskiego 27
50-370 Wroclaw, Poland
Fax: +48 71 3202656
E-mail: robert.lukomski@pwr.wroc.pl